THE JOURNAL OF PHYSICAL CHEMISTRY Letters

Perspective

pubs.acs.org/JPCL

Magnetic Particle Imaging Tracers: State-of-the-Art and Future Directions

Lisa M. Bauer,[†] Shu F. Situ,[‡] Mark A. Griswold,[†,§] and Anna Cristina S. Samia*[,‡]

[†]Department of Physics, Case Western Reserve University, Cleveland, Ohio 44106, United States

[‡]Department of Chemistry, Case Western Reserve University, Cleveland, Ohio 44106, United States

[§]Department of Radiology, Case Western Reserve University and University Hospitals of Cleveland, Cleveland, Ohio 44106, United States

ABSTRACT: Magnetic particle imaging (MPI) is an emerging imaging modality with promising applications in diagnostic imaging and guided therapy. The image quality in MPI is strongly dependent on the nature of its iron oxide nanoparticle–based tracers. The selection of potential MPI tracers is currently limited, and the underlying physics of tracer response is not yet fully understood. An in-depth understanding of the magnetic relaxation processes that govern MPI tracers, gained through concerted theoretical and experimental work, is crucial to the development of optimized MPI tracers. Although tailored tracers will lead to improvements in image quality, tailored relaxation may also be exploited for biomedical applications or more flexible image contrast, as in the recent demonstration of color MPI.

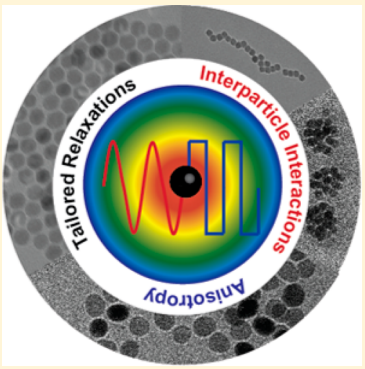

Magnetic particle imaging (MPI) is an exciting new imaging modality, first introduced by Gleich and Weizenecker in 2005.[1] MPI exploits the nonlinear magnetization of iron-based tracer nanoparticles to generate maps of tracer distribution.[2−5] Although it is still in the preclinical stage, there are several key features that motivate future development, such as excellent contrast, high signal-to-noise ratio (SNR) and the potential for high resolution imaging, as well as the safety profile of its tracers.[6−9] Over the past 10 years MPI has advanced rapidly, and initial studies suggest that it eventually may have a number of applications for human imaging, such as angiography, cell tracking, and cancer imaging.[9,10] Several preclinical MPI scanners are currently in operation, and efforts to advance hardware toward human imaging are ongoing. In parallel with hardware development, there is a great need for tailored MPI tracers, making MPI of particular interest to the Physical Chemistry community. MPI is the first imaging modality to be driven by tracer development. As such, its future success depends heavily on advances in nanoparticle fabrication and theoretical models of nanoscale magnetization.

MPI is the first imaging modality to be driven by tracer development. As such, its future success depends heavily on advances in nanoparticle fabrication and theoretical models of nanoscale magnetization.

MPI has the potential to be highly competitive in terms of image quality and quantitative ability, meeting or exceeding the contrast, sensitivity, and spatial and temporal resolution of established clinical techniques such as positron emission tomography (PET), magnetic resonance imaging (MRI), and computed tomography (CT).[11,12] As there is no background signal from tissue, MPI has excellent contrast, and because it utilizes low-frequency magnetic fields, it has no depth attenuation. Additionally, MPI's theoretically achievable spatial resolution is on the order of 200−500 μm, and it shows promise as a real-time imaging modality, with a temporal resolution of seconds−minutes.[3,11] Some published studies have predicted that MPI may have a sensitivity on par with PET, approximately 10^{-11}−10^{-12} M, requiring only nanograms of tracer material to produce an image.[11] Early imaging experiments have achieved a sensitivity of ∼200 nanograms of iron per voxel, which corresponds to a sensitivity of roughly 2×10^{-6} M, though advances in hardware and tracer design could push this limit closer to 10^{-7}−10^{-8} M.[13] However, when drawing comparisons between MPI and nuclear imaging, it may be more instructive to consider dose-limited sensitivity. Nuclear imaging techniques, such as PET and SPECT, require a radioisotope tracer and are limited in the administered dosage. MPI, which uses iron-based tracers, is not subjected to such a stringent dose limitation, and may one day surpass the dose-limited sensitivity of nuclear imaging techniques.

MPI is also considered to be a safe imaging modality with many potential clinical applications. The tracers used in MPI

Received: March 23, 2015
Accepted: June 11, 2015
Published: June 17, 2015

DOI: 10.1021/acs.jpclett.5b00610
J. Phys. Chem. Lett. 2015, 6, 2509−2517

serve as a safer alternative to the current iodine- and gadolinium-based tracers used in CT and MRI scans, especially for patients with chronic kidney disease (CKD).[14,15] MPI could thereby circumvent the risks associated with contrast-enhanced imaging of patients with CKD due to its use of iron-based tracers, which are known to be cleared through the liver, and have even received FDA approval for the treatment of anemia.[16] MPI has also been proposed for cardiovascular interventional imaging, and the first signal-generating instruments for that purpose have been characterized.[17] Moreover, MPI's quantitative nature suggests that it may be a viable cell tracking technique.[8,18] As an MPI image reflects only tracer distribution, and is thus similar to a PET image, MPI may also prove useful as a cancer imaging method, especially as many preclinical cancer imaging agents are iron-based.

In this paper, we present an introduction to the MPI imaging process and the physics of MPI tracers. We discuss current magnetic relaxation theory and optimization of tracers for MPI, as well as open questions and related therapeutic applications that may be exploited for MPI. In particular, we note a key point: that the success of MPI is heavily reliant on a suitable tracer, and the field of tracer development opens up new opportunities for iron-based tracer design.

We note a key point: that the success of MPI is heavily reliant on a suitable tracer, and the field of tracer development opens up new opportunities for iron-based tracer design.

The MPI Process. MPI is driven by the physics of its tracers, which are typically superparamagnetic iron oxide nanoparticles (SPIONs). The SPIONs used in MPI are characterized by Langevin magnetization, and their magnetization (M) as a function of applied magnetic field $H(t)$ is given by the Langevin equation

$$M(H(t)) = m_s\left(\coth(\alpha H(t)) - \frac{1}{\alpha H(t)}\right)$$

where

$$\alpha = \frac{\mu_0 m_s}{k_B T}$$

and c is the tracer concentration, μ_0 is the permeability of free space, m_s is the saturation magnetic moment, k_B is the Boltzmann constant, and T is temperature.[6] The saturation magnetic moment is given by

$$m_s = \frac{\pi d_c^3 M_s}{6}$$

where d_c is the magnetic core diameter, and M_s is the saturation magnetization of the tracer. Single-core MPI tracers are usually very close to the ferromagnetic transition size range, which generally falls within 20−30 nm diameter.

There are two established methods for MPI: harmonic-space (also known as frequency-space) and x-space. Though there are differences between the two techniques, both generate a signal by exploiting the magnetization curve of SPION tracers for excitation and selective saturation, as illustrated in Figure 1a−b.[1] As illustrated in Figure 1b, a static magnetic field gradient generates a field free point (FFP)—a single location in space at which the magnetic field is zero. When a time-varying magnetic field is superimposed, only those SPIONs in the FFP generate a time-varying magnetization, as SPIONs elsewhere are magnetically saturated. This time-varying magnetization induces a voltage in a nearby receiver coil (Figure 1c). The raw MPI signal is obtained by sweeping the FFP over the imaging field of view (FOV), and image reconstruction techniques generate a map of tracer concentration (Figure 1d).

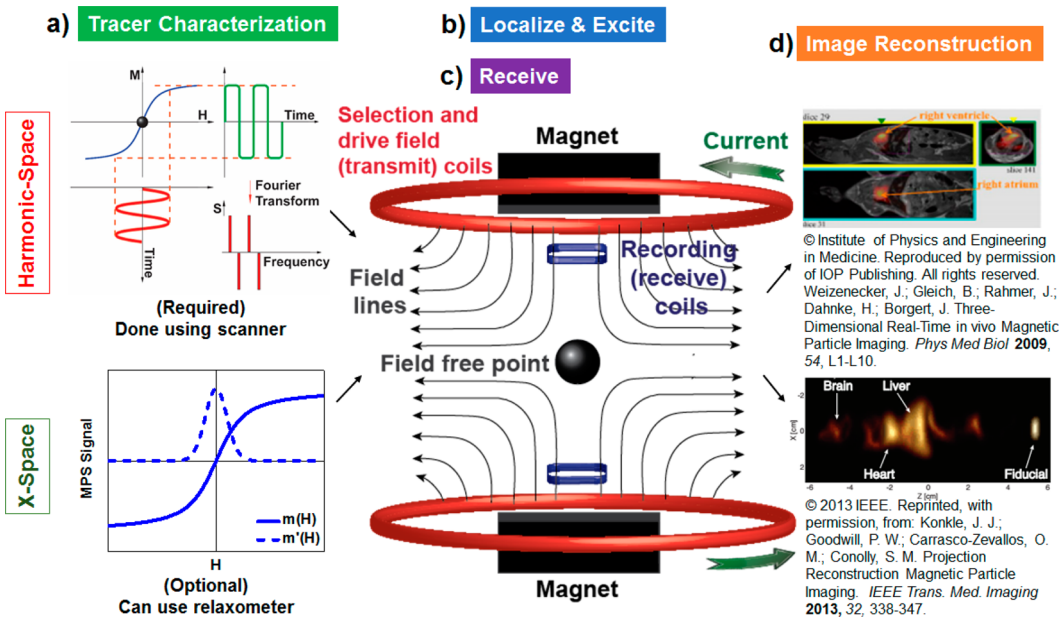

Figure 1. Schematic representation of the MPI image generation workflow, comparing harmonic-space and x-space MPI. The MPI image generation process can be divided into four steps: (a) tracer selection and characterization, (b) excitation and spatial localization, (c) signal reception, and (d) image reconstruction. Although some of these steps differ between harmonic-space and x-space MPI the scanner geometry is consistent between the two methods.

DOI: 10.1021/acs.jpclett.5b00610
J. Phys. Chem. Lett. 2015, 6, 2509−2517

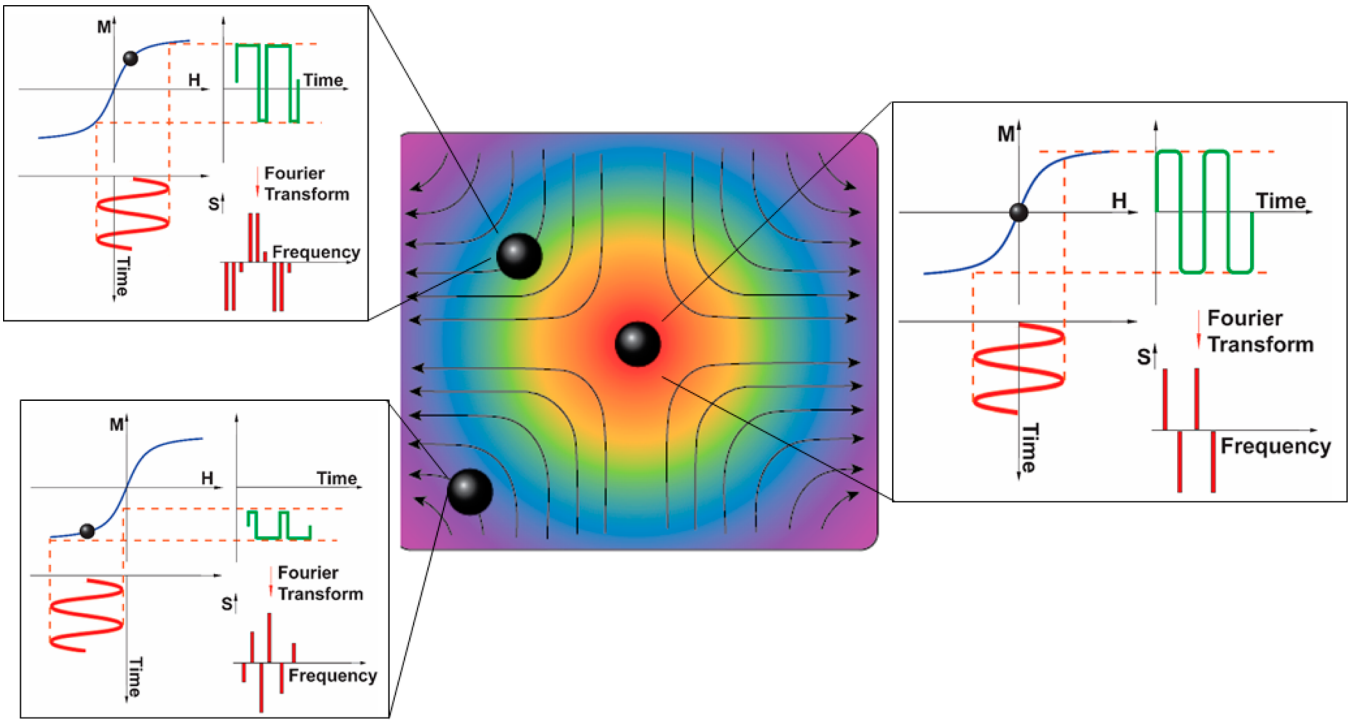

Figure 2. In harmonic-space MPI, the first step is acquisition of the system function, which contains the spectral response of tracers at every location within the field of view. This calibration scan is then used for image reconstruction.

The seminal MPI images, including the first in vivo imaging of a beating mouse heart, were generated using harmonic-space reconstruction,[1,3] The fundamental signal of harmonic-space MPI is the set of harmonic amplitudes obtained by calculating the Fourier transform of the tracer's time-dependent magnetization. Harmonic-space MPI requires initialization by construction of a "system matrix."[19] The system matrix contains the spectral response of an idealized point source tracer at every location in the imaging FOV as illustrated in Figure 2. The FFP is typically swept through the FOV in a Lissajous pattern, using a combination of drive fields and focus (or selection) fields.[3] Image reconstruction is then performed using matrix inversion techniques.[20,21] Tracer characterization is accomplished using MPI spectroscopy, which measures the harmonic response of a tracer in the FFP, and the resulting set of harmonics can be used to gauge the behavior of a potential MPI tracer.[22]

The second MPI technique is known as *x*-space MPI.[6,7] *X*-space MPI is linear and shift-invariant, a property essential to quantitative medical imaging, and has been proven to be mathematically equivalent to the system matrix approach.[23] Although the fundamental scanner geometry of *x*-space MPI is shared with harmonic-space MPI, the *x*-space signal corresponds to a temporal scan through *x*-space, rather than a set of harmonics, and *x*-space MPI does not require any precharacterization of the tracer. Signal generation can be summarized as follows: as the magnetic field is swept from negative to positive (or vice versa) across a SPION (corresponding to FFP movement), it induces a magnetization flip that is detected in a nearby receiver coil. The shape of this signal is the derivative of the magnetization curve and is the point spread function [PSF, $h(x)$] of the *x*-space MPI system. Spatial localization is achieved using the same gradients as harmonic-space MPI, and image reconstruction is achieved by gridding the raw signal to the known FFP trajectory (after velocity compensation). The *x*-space MPI image is essentially a convolution of the PSF with the spatial distribution of tracer material (Figure 3).[6,7] Once the PSF is known, image quality can be predicted to a great degree of accuracy.

Tracer development is central to the advancement of MPI, as key factors such as resolution and SNR are governed by hardware and tracer properties. The resolution is a function of both gradient strength and particle characteristics, and is given as

$$\Delta x = \frac{24 k_B T}{\pi \mu_0 M_s G d_C^3}$$

where G is the gradient strength, and ideal, Langevin particles are assumed.[7,19] From this equation, it would appear that increasing gradient strength and particle diameter would improve resolution without bound. In theory, increasing the diameter of a nanoparticle from 17 to 25 nm leads to a greater than 3-fold improvement in resolution, though in practice this gain is limited by the physics of magnetic relaxation.

Magnetic Relaxation in MPI. The Langevin picture of the magnetization process provides an incomplete picture as it assumes an instantaneous response of a SPION to a change in magnetic field and, thus, ignores magnetic relaxation effects. In order to align with an external magnetic field, SPIONs must overcome thermal and viscous forces that depend on a combination of the SPIONs' crystal structure, environment, and experimental measurement parameters. In general, MPI tracers may achieve a magnetic reversal by Brownian rotational diffusion, Néel relaxation, or hysteretic reversal (Figure 4). Brownian rotation diffusion (also termed "Brownian relaxation" or "magnetoviscous relaxation" in MPI literature) refers to the physical rotation of the magnetically blocked tracer with respect to surrounding fluid. The time constant associated with Brownian relaxation is given by

$$\tau_B = \frac{3 V_H \eta}{k_B T}$$

DOI: 10.1021/acs.jpclett.5b00610
J. Phys. Chem. Lett. 2015, 6, 2509−2517

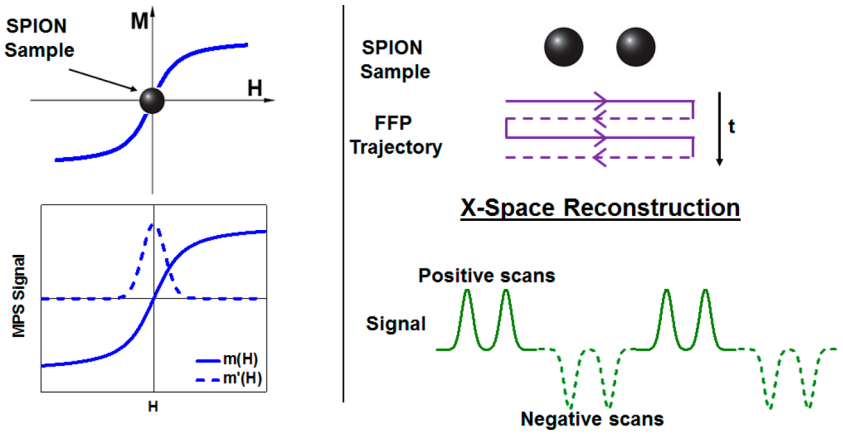

Figure 3. Overview of *x*-space MPI. The point spread function (PSF) of the *x*-space MPI image is the derivative of the tracer's magnetization curve. The *x*-space MPI process is a temporal scan through the field of view: as the FFP passes over a nanoparticle, it induces a magnetization flip that is detected by a receiver coil, and the received signal is gridded to the known FFP trajectory to produce an image.

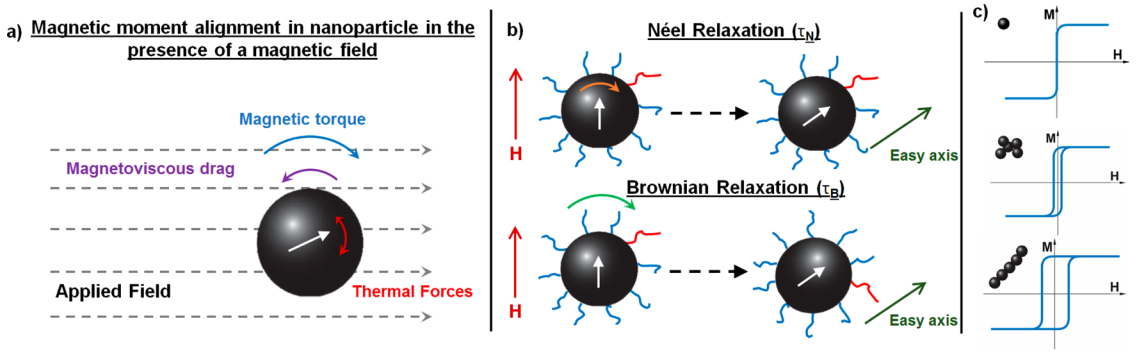

Figure 4. When exposed to an external magnetic field, SPIONs are subject to relaxation mechanisms and must overcome both thermal forces and viscous drag forces to align with the applied field (a). For tracers used in MPI, relaxation is typically a combination of Brownian and Néel relaxation (b). A third form of relaxation occurs in nanoparticles or clusters with nonzero coercivity (c).

where, V_H is the hydrodynamic volume of the tracer, η is the viscosity of the surrounding fluid, k_B is Boltzmann's constant, and T is temperature.[24]

Néel relaxation occurs when the thermal energy overcomes the anisotropy energy barrier, leading to a rotation of the internal magnetic moment, rather than a physical rotation of the tracer. The Néel relaxation time constant is given by

$$\tau_N = \tau_0 e^{KV_c/k_BT}$$

where K is the crystalline anisotropy constant, V_C is the volume of the magnetic core, and τ_0 is a time constant on the order of 10^{-10} s.[25] A third possible form of relaxation is hysteretic reversal, found in tracers or clusters with nonzero coercivity.[26]

Understanding relaxation in MPI requires consideration of the magnetic fields (DC and AC) present during an imaging experiment. The conventional relaxation times are only appropriate for low-amplitude magnetic fields that are much smaller than anisotropy field ($H_{applied} \ll H_K = 2K/M_s$), but an MPI tracer will always be exposed to a strong gradient magnetic field and time-varying excitation fields, on the order of 5 T/m and 40 mT peak-to-peak, respectively. Recent simulation work has investigated the dependence of Brownian and Néel relaxation times on magnetic field amplitude, suggesting that the current model of zero-field relaxation does not completely describe relaxation in the presence of the MPI system and may underestimate the Néel relaxation time by several orders of magnitude.[27]

It is well known that relaxation can simultaneously blur the image and diminish the overall SNR.[28] This effect is illustrated in Figure 5, the PSF is blurred asymmetrically in the scan direction (the direction the FFP would be moving across the voxel), and the peak signal is decreased. A specialized device, known as an *x*-space relaxometer, can be used to measure the one-dimensional PSF of a tracer.[29] Relaxometry facilitates efficient screening of potential MPI tracers and is also a useful tool for studying the physics of SPIONs.

Tailoring Tracers for MPI. MPI is novel in that it is a tracer-driven imaging modality, yet there are no commercially available, dedicated MPI tracers and the current "gold standard" tracer is Resovist (Bayer Schering Pharma AG, Berlin), a discontinued MRI contrast agent. Although it is the benchmark by which all potential tracers are evaluated, its successful performance is surprising; by all conventional reasoning, Resovist should not produce a good signal. The manufacturer reports a 4 nm SPION diameter, which by standard Langevin theory would lead to a poor resolution. Gleich et al. suggest that less than 3% of particles actually contribute to the MPI signal, the small fraction of large-diameter particles.[1] A TEM of Resovist clearly indicates polydispersity, and Eberbeck et al. suggest that Resovist's performance may be due in part to a bimodal size distribution, leading to nanoparticle clusters that outperform single-core nanoparticles.[30] Although Resovist has so far been an experimentally successful tracer, a tailored MPI tracer could lead to significant gains in SNR and resolution.

DOI: 10.1021/acs.jpclett.5b00610
J. Phys. Chem. Lett. 2015, 6, 2509−2517

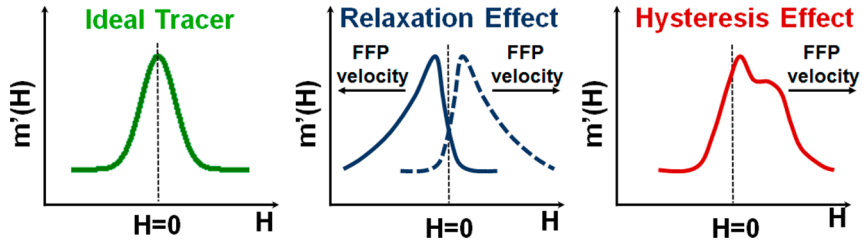

Figure 5. Effect of relaxation on the PSF. Relaxation causes a shift in the location of the peak, as well as blurring in the scan direction (the direction that the FFP is moving). Hysteresis leads to a shoulder in the PSF.

Designing tracers specifically for MPI is an emerging but important area of research, as tracer optimization is key to improving sensitivity and resolution.[8] Early work on core size optimization suggests that there exists an optimal nanoparticle for each operating frequency (f). This is driven by the transition from Néel to Brownian relaxation dominance, or when the effective relaxation time constant approaches $1/2\pi f$.[31,32] Ferguson et al. recently demonstrated this effect using spectroscopy and relaxometry at 25 kHz, for which the optimal core diameter was determined to be 20 nm.[33]

A more recent work by Ferguson et al. presents a thorough imaging study using tailored monodisperse, 26−28 nm single-core tracers with PEG-based coatings.[34] One tailored tracer achieved signal intensity gains of 2−3× compared to Resovist, in both harmonic-space and x-space MPI images. A second tailored tracer (with larger hydrodynamic diameter) outperformed Resovist in a resolution phantom study. Points separated by 2.7 mm were resolved using Resovist, as compared to a 1.7 mm resolution using the tailored tracer.[34] Although this is a great improvement, relaxometry measurements of the tailored tracer predicted a spatial resolution of 0.7 mm. The authors note that this discrepancy is not fully understood but may be related to tracer behavior in the multidimensional magnetic fields in the MPI scanner. It is also interesting to note that the authors observed hysteresis under typical magnetic fields found in MPI, which is consistent with simulations from Weizenecker et al. that suggest a small core anisotropy and coercivity may enhance MPI performance of a SPION tracer.[35]

Magnetic field parameters (amplitude, frequency) have been shown to affect tracer response. Shah, Ferguson, and Krishnan examined the effect of changing the slew rate of the magnetic field, ωH_0, the product of the angular frequency and drive field amplitude.[36] The authors used tracers with a core diameter of ∼26 nm and hydrodynamic diameter of ∼70 nm. When the slew rate was held constant, the signal from MPI tracers (both fluid and immobilized by freezing) was unchanged. There were differences between fluid and immobilized samples due to restricted Brownian relaxation, though these differences were relatively small. In fluid samples, the authors observed an increase in coercivity and hysteresis loop area with slew rate. The MPI signal showed a strong dependence on field amplitude, with low-amplitude magnetic fields generating minor hysteresis loops. For a constant frequency of 26 kHz, low-amplitude fields produced the best MPI signal. On the basis of the safety limits calculated by Saritas et al., this may be optimal for human imaging, though a smaller field amplitude does limit the imaging field of view and could require more complicated imaging protocols.[37]

Designing tracers for in vivo use requires consideration of circulation time, biodistribution, and cell uptake.[38,39] Resolution improves with core size, so a magnetic core size just below the ferromagnetic limit is preferred for high resolution. This is complicated by the need for a surfactant coating to promote biocompatibility, as the increase in hydrodynamic size increases the effect of viscous relaxation, so core size must be optimized in tandem with the surfactant. The surfactant should be thin to minimize viscous relaxation, but thick enough to prevent aggregation, a common problem in nanoparticle synthesis. Care should be taken to determine if significant aggregation exists within a sample, as it is known to cause changes in the MPI signal. Ludwig et al. have demonstrated the use of dynamic measurements in detecting aggregates, which standard TEM and dynamic light scattering (DLS) measurements can miss.[40] Tracer stability is another critical concern for imaging experiments. Long-term cell tracking studies require tracers that are stable over days or weeks in what can be harsh environments. Highly acidic environments are known to degrade tracers in a short period of time, weakening their MPI performance, which motivates the development of new surface modifications.[41]

In addition to experimental investigation of relaxation, a number of groups are developing theoretical models. Dhavalikar and Rinaldi have recently presented results from rotational Brownian dynamics simulations that model hydrodynamic, magnetic, and thermal torques on a collection of noninteracting magnetic nanoparticles.[42] This is an excellent start to a relaxation model and could be expanded to include factors such as polydispersity, anisotropy, and particle−particle interactions. Dipole−dipole interactions have been modeled for hyperthermia, using the Landau−Lifshitz−Gilbert equation and Langevin dynamics, and should be considered for MPI simulations, especially for multicore tracers or those that aggregate.[43]

One of the challenges to MPI simulations is the absence of a readily accessible method for measuring the anisotropy constant K. Small variations of this value can lead to orders-of-magnitude variations in relaxation simulations and difficulties in matching results to experimental data. A more accessible anisotropy measurement technique, one that fits within the workflow of a relaxometry experiment, would facilitate easier comparison of MPI simulations to relaxometry data. There are a number of complementary techniques for characterizing nanoparticles, including AC susceptometry, magnetorelaxometery, and spectroscopy. The combined use of all three, such as in the study by Ludwig et al., can be of great help in understanding nanoparticle properties and MPI performance.[44]

Along with simulations, spectroscopy and relaxometry for high-throughput screening, it would be advantageous to have a platform for tracer development, particularly for investigating Néel relaxation. Pablico-Lansigan et al. have developed nanocomposites that restrict relaxation to the Néel mechanism (Figure 6).[12] The nanocomposites are a mixture of magnetite nanoparticles and ultrahigh molecular weight polyethylene (UHMWPE) that has been compressed into a thin, flexible film.

DOI: 10.1021/acs.jpclett.5b00610
J. Phys. Chem. Lett. 2015, 6, 2509−2517

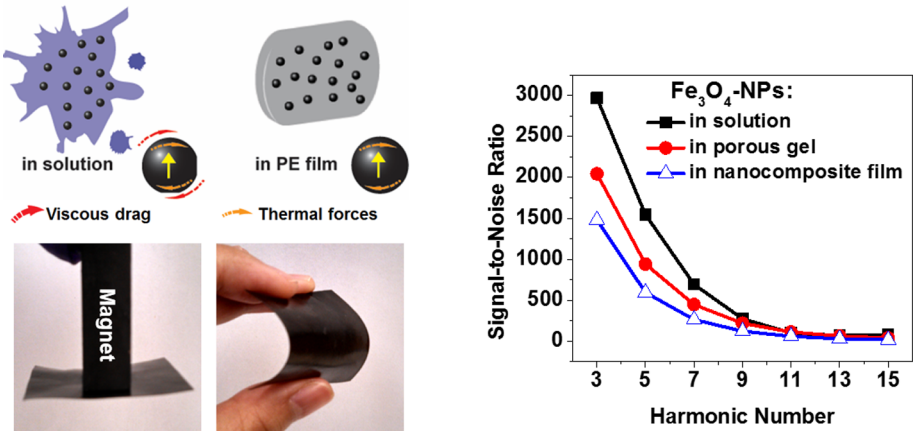

Figure 6. Nanoparticles in the nanocomposite films are immobilized, and their main mode of magnetic relaxation is Néel. Such immobilization leads to a decrease in signal-to-noise ratio as compared to nanoparticles in solution or in a porous gel, as measured by MPI Spectroscopy. (Unpublished Data.)

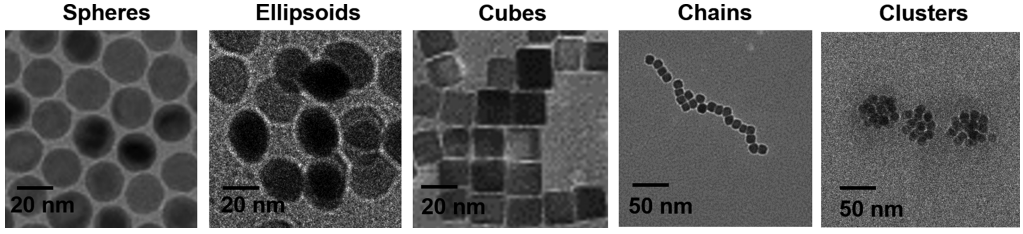

Figure 7. Transmission electron microscope (TEM) images of nanoparticle platforms under development in our group. (Unpublished data.)

Initially proposed as an alternative to current hip prostheses, the nanocomposites may also be useful for developing nanoparticles that are to be imaged in a bound state (for example, targeted nanoparticles) or as a fiducial marker for coregistering MPI images with anatomic reference images.

New Directions. The discussion presented here represents great progress toward developing MPI tracers. We note, however, that much of tracer development seems to be focused on creating a *single* ideal nanoparticle for MPI, a one-size-fits-all solution for imaging, but the concept of an ideal tracer is too limiting. Two of MPI's potential applications—angiography and cell tracking—expose tracers to distinct biological environments. Angiography alone has great variability in vascular environments, as blood velocity varies over 3 orders of magnitude between major vessels and capillaries and shear stress varies with vessel size. The MPI signal is very sensitive to a nanoparticle's local environment, particularly for larger particles (>20 nm).[26] Rauwerdink et al. have exploited this property for quantification of molecular binding.[45] It is possible that such a technique could lead to in vivo measurements of bound fractions, or functional image contrast.

In addition to developing new, tailored tracers specifically for MPI, the MPI community should take advantage of the design and fabrication practices used to create SPIONs for biomedical applications in order to develop specialized tracers. SPIONs have long been exploited in magnetic hyperthermia and drug delivery applications and have been used as contrast agents for MRI.[46−48] There already exists a collection of interesting magnetic nanoparticle structures and assemblies, none of which have yet been investigated in the context of MPI.

To date, the spherical SPION is most commonly used in MPI tracer optimization studies. Exploring SPIONs of different shapes is highly interesting due to their increase in shape anisotropy, which can ultimately influence their magnetic relaxation properties. Previous studies by Lee et al., Macher et al., and Noh et al. have demonstrated nonspherical nanoparticles have significantly enhanced performance in MRI and magnetic hyperthermia for tumor ablation due to their increase in shape anisotropy compared to their spherical counterparts.[49−51] Optimizations of spherical, ellipsoidal, and cubic iron oxide nanoparticles are currently underway in our laboratories for their respective MPI performance (Figure 7). Furthermore, higher-order structures of SPIONs, such as chains and clusters, can expand our ability to study the effect of interparticle interactions on magnetic relaxation. Higher-order nanostructures have shown promising potentials in the areas of drug delivery and imaging owing to their unique architecture.[52−54] MPI relaxometry can be an excellent tool to better understand the underlying physics and magnetic relaxation mechanisms of these structures.

One particularly exciting development is the concept of "color" MPI (cMPI): the ability to disentangle signals from multiple, unique tracers that are colocalized. Rahmer et al. have published the first experimental evidence of color MPI, distinguishing between Resovist and Ferudextran, in diluted and dried forms (Figure 8).[55] Though there exists a great similarity between the three materials used, a good degree of signal distinction was achieved in the resulting images. It would be advantageous to add a degree of orthogonality between SPIONs, either in size or formulation, or in the experimental parameters, such as drive fields of different amplitudes or frequencies. Whether or not image reconstruction problems or relaxation effects can be circumvented has yet to be demonstrated experimentally, but the potential applications of color MPI warrant further study; such a development would be highly useful for cell tracking and drug-delivery studies, as well as in vivo distribution dynamics of SPION tracers.

DOI: 10.1021/acs.jpclett.5b00610
J. Phys. Chem. Lett. 2015, 6, 2509−2517

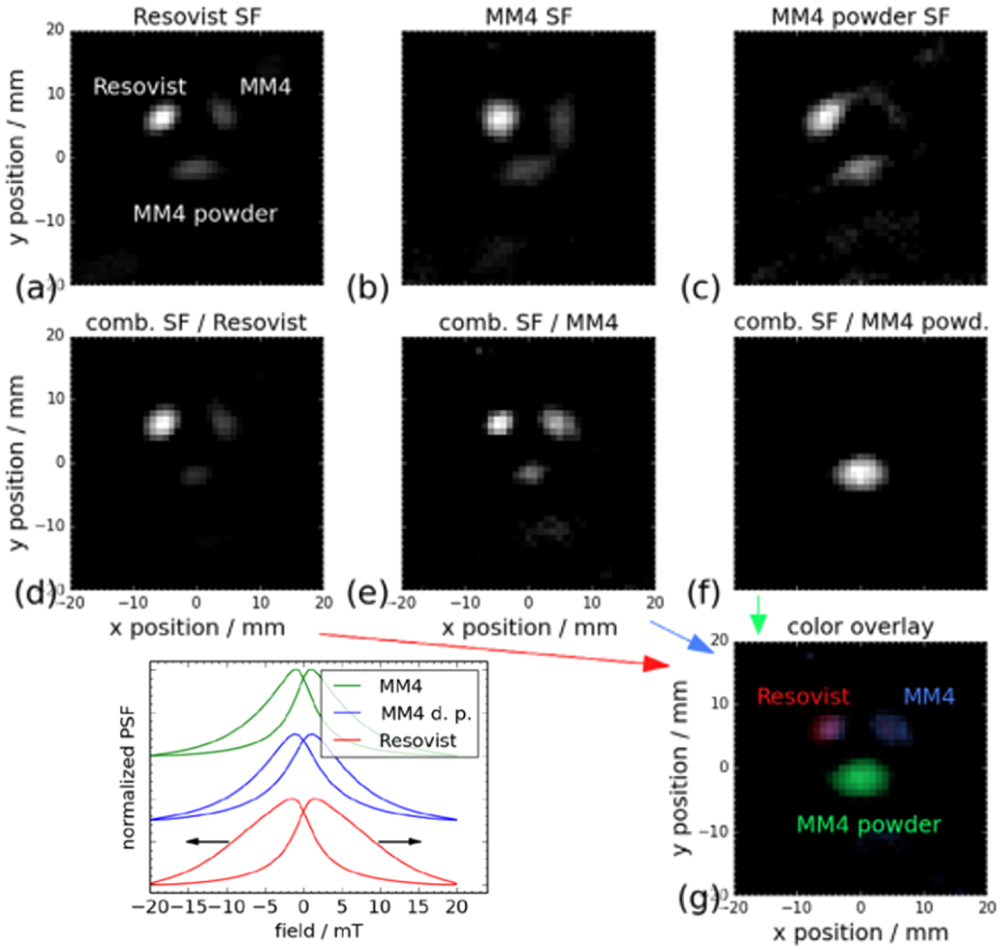

Figure 8. Experimental demonstration of color MPI. Point spread functions from three tracers are different due to hysteresis effects. Image reconstruction using individual system functions (SF) results in distorted images (a)−(c), but the use of combined SFs achieves better separation between tracers (d)−(f). A color overlay of scaled figures (d)−(f) is shown in figure (g). Copyright 2015, Institute of Physics and Engineering in Medicine (Rahmer, J.; Halkola, A.; Gleich, B.; Schmale, I.; Borgert, J. First experimental evidence of the feasibility of multicolor magnetic particle imaging. *Phys. Med. Biol.* **2015**, *60*, 1775−1791.). Reproduced with permission of IOP Publishing.

Future Directions. Much work remains before MPI can be regarded as a competitive clinical imaging modality. Although there are several preclinical research scanners, MPI faces the challenge of scaling hardware to human imaging. Though the magnetic fields used in MPI are generally considered safe, there are still physiological limits of peripheral nerve stimulation and tissue heating (specific absorption rate, SAR) that place bounds on gradient strength and frequency.[37] There are no fundamental limits that would prevent scaling MPI to human imaging, so though it may be an engineering challenge, it is theoretically feasible. In parallel with scanner development, many groups are working toward making tracer characterization more sensitive. The importance of careful tracer characterization cannot be overstated, and MPI spectroscopy and relaxometry must match the conditions of the imaging environment, in terms of magnetic fields, frequencies, and shielding from external sources of interference. Further, more sensitive measurements enable applications development, such as targeting studies, in which significant SNR loss can be expected due to significant relaxation.

The progress in MPI over the last 10 years is certainly very exciting, but the field is still young and there are many open questions. Though it is a tracer-driven imaging technique, the physics of MPI tracers is still not completely understood, and the field of tracer development is still emerging. MPI may be able to take advantage of the existing collection of SPIONs developed for biomedical applications, especially for the purpose of achieving functional contrast. MPI shows great promise as a safe, high-resolution, real-time imaging technique, and has, at the preclinical stage, shown promise for angiography and cell tracking, but its future success will heavily rely on the availability of optimized tracers.

MPI shows great promise as a safe, high-resolution, real-time imaging technique, and has, at the preclinical stage, shown promise for angiography and cell tracking, but its future success will heavily rely on the availability of optimized tracers.

AUTHOR INFORMATION

Corresponding Author
*E-mail: anna.samia@case.edu.

DOI: 10.1021/acs.jpclett.5b00610
J. Phys. Chem. Lett. 2015, 6, 2509−2517

Notes

The authors declare no competing financial interest.

Biographies

Lisa M. Bauer is a Ph.D. candidate in the Department of Physics at Case Western Reserve University. She received her B.A. in Physics in 2009 and M.S. in Physics Entrepreneurship in 2010, both from CWRU. Her current research is focused on developing hardware for magnetic particle relaxometry.

Shu F. Situ received her B.S. Chemistry degree from the University of Michigan in 2011 and is currently a Ph.D. candidate in the Department of Chemistry at CWRU. Her research interests focus on the synthesis of iron oxide nanoparticles with tunable anisotropy and magnetic relaxation for magnetic particle imaging.

Mark A. Griswold is a Professor in the Department of Radiology at CWRU and University Hospitals of Cleveland. He obtained his Ph.D. degree from Universität Würzburg in Würzburg, Germany. His research focuses primarily on the development of software and hardware for fast MRI and MPI imaging methods.

Anna Cristina S. Samia is an Assistant Professor in the Department of Chemistry at CWRU. She obtained her Ph.D. degree from the Georgia Institute of Technology and her Postdoctoral training at Argonne National Laboratory. Her research centers on the fabrication of magnetic nanoparticles and their composites for MPI tracer development. More information about her laboratory may be found at caslabs.case.edu/samia/

■ ACKNOWLEDGMENTS

This work was supported in part by NCI Training Programs in Cancer Pharmacology 5R25 CA148052 (L.M.B.), NIH Interdisciplinary Biomedical Imaging Training Program T32EB007509 (L.M.B.), NIH 1R24MH106053-01 (M.A.G.), and an NSF-CAREER Grant (DMR-1253358) from the Solid State and Materials Chemistry Program (A.C.S.S.).

■ REFERENCES

(1) Gleich, B.; Weizenecker, J. Tomographic Imaging Using the Nonlinear Response of Magnetic Particles. *Nature* **2005**, *435*, 1214−7.
(2) Gleich, B.; Weizenecker, J.; Borgert, J. Experimental Results on Fast 2D-Encoded Magnetic Particle Imaging. *Phys. Med. Biol.* **2008**, *53*, N81−4.
(3) Weizenecker, J.; Gleich, B.; Rahmer, J.; Dahnke, H.; Borgert, J. Three-Dimensional Real-Time In Vivo Magnetic Particle Imaging. *Phys. Med. Biol.* **2009**, *54*, L1−L10.
(4) Goodwill, P. W.; Konkle, J. J.; Zheng, B.; Saritas, E. U.; Conolly, S. M. Projection *X*-space Magnetic Particle Imaging. *IEEE Trans. Med. Imaging* **2012**, *31*, 1076−1085.
(5) Konkle, J. J.; Goodwill, P. W.; Carrasco-Zevallos, O. M.; Conolly, S. M. Projection Reconstruction Magnetic Particle Imaging. *IEEE Trans. Med. Imaging* **2013**, *32*, 338−347.
(6) Goodwill, P. W.; Conolly, S. M. The *X* Space Formulation of the Magnetic Particle Imaging Process: One-Dimensional Signal, Resolution, Bandwidth, SNR, SAR and Magnetostimulation. *IEEE Trans. Med. Imaging* **2009**, *29*, 1851−1859.
(7) Goodwill, P. W.; Conolly, S. M. Multidimensional *X*-space Magnetic Particle Imaging. *IEEE Trans. Med. Imaging* **2011**, *30*, 1581−1590.
(8) Goodwill, P. W.; Saritas, E. U.; Croft, L. R.; Kim, T. N.; Krishnan, K. M.; Schaffer, D. V.; Conolly, S. M. *X*-space MPI: Magnetic Nanoparticles for Safe Medical Imaging. *Adv. Mater.* **2012**, *24*, 3870−3877.
(9) Saritas, E. U.; Goodwill, P. W.; Croft, L. R.; Konkle, J. J.; Lu, K.; Zheng, B.; Conolly, S. M. Magnetic Particle Imaging (MPI) for NMR and MRI Researchers. *J. Magn. Reson.* **2013**, *229*, 116−26.
(10) Rahmer, J.; Antonelli, A.; Sfara, C.; Tiemann, B.; Gleich, B.; Magnani, M.; Weizenecker, J.; Borgert, J. Nanoparticle Encapsulation in Red Blood Cells Enables Blood-Pool Magnetic Particle Imaging Hours After Injection. *Phys. Med. Biol.* **2013**, *58*, 3965−77.
(11) Krishnan, K. M. Biomedical Nanomagnetics: A Spin Through Possibilities in Imaging, Diagnostics, and Therapy. *IEEE Trans. Magn.* **2010**, *46*, 2523−2558.
(12) Pablico-Lansigan, M. H.; Situ, S. F.; Samia, A.C.S. Magnetic Particle Imaging: Advancements and Perspectives for Real-Time In Vivo Monitoring and Image-Guided Therapy. *Nanoscale* **2013**, *5*, 4040−55.
(13) Goodwill, P. W.; Lu, K.; Zheng, B.; Conolly, S. M. An *X*-space Magnetic Particle Imaging Scanner. *Rev. Sci. Instrum.* **2012**, *83*, 033708.
(14) Goldfarb, S.; McCullough, P. A.; McDermott, J.; Gay, S. B. Contrast-Induced Acute Kidney Injury: Specialty-Specific Protocols for Interventional Radiology, Diagnostic Computed Tomography Radiology, and Interventional Cardiology. *Mayo Clin. Proc.* **2009**, *84*, 170−179.
(15) Abu-Alfa, A. K. Nephrogenic Systemic Fibrosis and Gadolinium-Based Contrast Agents. *Adv. Chronic Kidney Dis.* **2011**, *18*, 188−98.
(16) Lu, M.; Cohen, M. H.; Rieves, D.; Pazdur, R. FDA report: Ferumoxytol for Intravenous Iron Therapy in Adult Patients with Chronic Kidney Disease. *Am. J. Hematol.* **2010**, *85*, 315−9.
(17) Haegele, J.; Biederer, S.; Wojtczyk, H.; Graser, M.; Knopp, T.; Buzug, T. M.; Barkhausen, J.; Vogt, F. M. Toward Cardiovascular Interventions Guided by Magnetic Particle Imaging: First Instrument Characterization. *Magn. Reson. Med.* **2013**, *69*, 1761−7.
(18) Markov, D. E.; Boeve, H.; Gleich, B.; Borgert, J.; Antonelli, A.; Sfara, C.; Magnani, M. Human Erythrocytes as Nanoparticle Carriers for Magnetic Particle Imaging. *Phys. Med. Biol.* **2010**, *55*, 6461−73.
(19) Rahmer, J.; Weizenecker, J.; Gleich, B.; Borgert, J. Signal Encoding in Magnetic Particle Imaging: Properties of the System Function. *BMC Medical Imaging* **2009**, *9*, 4.
(20) Knopp, T.; Rahmer, J.; Sattel, T. F.; Biederer, S.; Weizenecker, J.; Gleich, B.; Borgert, J.; Buzug, T. M. Weighted Iterative Reconstruction for Magnetic Particle Imaging. *Phys. Med. Biol.* **2010**, *55*, 1577−89.
(21) Rahmer, J.; Weizenecker, J.; Gleich, B.; Borgert, J. Analysis of a 3-D System Function Measured for Magnetic Particle Imaging. *IEEE Trans. Med. Imaging* **2012**, *31*, 1289−1299.
(22) Biederer, S.; Knopp, T.; Sattel, T. F.; Lüdtke-Buzug, K.; Gleich, B.; Weizenecker, J.; Borgert, J.; Buzug, T. M. Magnetization Response Spectroscopy of Superparamagnetic Nanoparticles for Magnetic Particle Imaging. *J. Phys. D: Appl. Phys.* **2009**, *42*, 205007.
(23) Lu, K.; Goodwill, P. W.; Saritas, E. U.; Zheng, B.; Conolly, S. M. Linearity and Shift Invariance for Quantitative Magnetic Particle Imaging. *IEEE Trans. Med. Imaging* **2013**, *32*, 1565−1575.
(24) Shliomis, M. I. Magnetic Fluids. *Phys.−Usp.* **1974**, *17*, 153−169.
(25) Brown, W. F., Jr. Thermal Fluctuations of a Single Domain Particle. *Phys. Rev.* **1963**, *130*, 1677−1686.
(26) Arami, H.; Ferguson, R. M.; Khandhar, A. P.; Krishnan, K. M. Size-Dependent Ferrohydrodynamic Relaxometry of Magnetic Particle Imaging Tracers in Different Environments. *Med. Phys.* **2013**, *40*, 071904.
(27) Deissler, R. J.; Wu, Y.; Martens, M. A. Dependence of Brownian and Neel Relaxation Times on Magnetic Field Strength. *Med. Phys.* **2014**, *41*, 012301.
(28) Croft, L. R.; Goodwill, P. W.; Conolly, S. M. Relaxation in *X*-space Magnetic Particle Imaging. *IEEE Trans. Med. Imaging* **2012**, *31*, 2335−2342.
(29) Goodwill, P. W.; Tamrazian, A.; Croft, L. R.; Lu, C. D.; Johnson, E. M.; Pidaparthi, R.; Ferguson, R. M.; Khandhar, A. P.; Krishnan, K. M.; Conolly, S. M. Ferrohydrodynamic Relaxometry for Magnetic Particle Imaging. *Appl. Phys. Lett.* **2011**, *98*, 262502.
(30) Eberbeck, D.; Wiekhorst, F.; Wagner, S.; Trahms, L. How the Size Distribution of Magnetic Nanoparticles Determines Their Magnetic Particle Imaging Performance. *Appl. Phys. Lett.* **2011**, *98*, 182502.

DOI: 10.1021/acs.jpclett.5b00610
J. Phys. Chem. Lett. 2015, 6, 2509−2517

(31) Ferguson, R. M.; Minard, K. R.; Khandhar, A. P.; Krishnan, K. M. Optimizing Magnetite Nanoparticles for Mass Sensitivity in Magnetic Particle Imaging. *Med. Phys.* **2011**, *38*, 1619.
(32) Ferguson, R. M.; Minard, K. R.; Krishnan, K. M. Optimization of Nanoparticle Core Size for Magnetic Particle Imaging. *J. Magn. Magn. Mater.* **2009**, *321*, 1548−1551.
(33) Ferguson, R. M.; Khandhar, A. P.; Krishnan, K. M. Tracer Design for Magnetic Particle Imaging (Invited). *J. Appl. Phys.* **2012**, *111*, 7B318−7B3185.
(34) Ferguson, R. M.; Khandhar, A. P.; Kemp, S. J.; Arami, H.; Saritas, E. U.; Croft, L. R.; Konkle, J.; Goodwill, P. W.; Halkola, A.; Rahmer, J.; et al. Magnetic Particle Imaging with Tailored Iron Oxide Nanoparticle Tracers. *IEEE Trans. Med. Imaging* **2014**, *34*, 1077−1084.
(35) Weizenecker, J.; Gleich, B.; Rahmer, J.; Borgert, J. Micro-Magnetic Simulation Study on the Magnetic Particle Imaging Performance of Anisotropic Mono-Domain Particles. *Phys. Med. Biol.* **2012**, *57*, 7317−27.
(36) Shah, S. A.; Ferguson, R. M.; Krishnan, K. M. Slew-Rate Dependence of Tracer Magnetization Response in Magnetic Particle Imaging. *J. Appl. Phys.* **2014**, *116*, 163910.
(37) Saritas, E. U.; Goodwill, P. W.; Zhang, G. Z.; Conolly, S. M. Magnetostimulation Limits in Magnetic Particle Imaging. *IEEE Trans. Med. Imaging* **2013**, *32*, 1600−1610.
(38) Khandhar, A. P.; Ferguson, R. M.; Arami, H.; Krishnan, K. M. Monodisperse Magnetite Nanoparticle Tracers for in vivo Magnetic Particle Imaging. *Biomaterials* **2013**, *34*, 3837−45.
(39) Lindemann, A.; Ludtke-Buzug, K.; Fraderich, B. M.; Grafe, K.; Pries, R.; Wollenberg, B. Biological Impact of Superparamagnetic Iron Oxide Nanoparticles for Magnetic Particle Imaging of Head and Neck Cancer Cells. *Int. J. Nanomedicine* **2014**, *9*, 5025−40.
(40) Ludwig, F.; Kuhlmann, C.; Wawrzik, T.; Dieckhoff, J.; Lak, A.; Kandhar, A. P.; Ferguson, R. M.; Kemp, S. J.; Krishnan, K. M. Dynamic Magnetic Properties of Optimized Magnetic Nanoparticles for Magnetic Particle Imaging. *IEEE Trans. Magn.* **2014**, *50*.
(41) Arami, H.; Krishnan, K. M. Intracellular Performance of Tailored Nanoparticle Tracers in Magnetic Particle Imaging. *J. Appl. Phys.* **2014**, *115*, 17B306.
(42) Dhavalikar, R.; Rinaldi, C. On the Effect of Finite Magnetic Relaxation on the Magnetic Particle Imaging Performance of Magnetic Nanoparticles. *J. Appl. Phys.* **2014**, *115*, 074308.
(43) Haase, C.; Nowak, U. Role of Dipole−Dipole Interactions for Hyperthermia Heating of Magnetic Nanoparticle Ensembles. *Phys. Rev. B* **2012**, *85*, 045435.
(44) Ludwig, F.; Remmer, H.; Kuhlmann, C.; Wawrzik, T.; Arami, H.; Ferguson, R. M.; Krishnan, K. M. Self-Consistent Magnetic Properties of Magnetite Tracers Optimized for Magnetic Particle Imaging Measured by AC Susceptometry, Magnetorelaxometry and Magnetic Particle Spectroscopy. *J. Magn. Magn. Mater.* **2014**, *360*, 169−173.
(45) Rauwerdink, A. M.; Weaver, J. B. Measurement of Molecular Binding Using the Brownian Motion of Magnetic Nanoparticle Probes. *Appl. Phys. Lett.* **2010**, *96*, 033702.
(46) Peiris, P. M.; Bauer, L.; Toy, R.; Tran, E.; Pansky, J.; Doolittle, E.; Schmidt, E.; Hayden, E.; Mayer, A.; Keri, R. A.; et al. Enhanced Delivery of Chemotherapy to Tumors Using a Multicomponent Nanochain with Radio-Frequency-Tunable Drug Release. *ACS Nano* **2012**, *6*, 4157−4168.
(47) Toy, R.; Bauer, L.; Hoimes, C.; Ghaghada, K. B.; Karathanasis, E. Targeted Nanotechnology for Cancer Imaging. *Adv. Drug Delivery Rev.* **2014**, *76*, 79−97.
(48) Kumar, C. S.; Mohammad, F. Magnetic Nanomaterials for Hyperthermia-Based Therapy and Controlled Drug Delivery. *Adv. Drug Delivery Rev.* **2011**, *63*, 789−808.
(49) Lee, N.; Choi, Y.; Lee, Y.; Park, M.; Moon, W. K.; Choi, S. H.; Hyeon, T. Water-Dispersible Ferrimagnetic Iron Oxide Nanocubes with Extremely High R(2) Relaxivity for Highly Sensitive In Vivo MRI of Tumors. *Nano Lett.* **2012**, *12*, 3127−31.
(50) Macher, T.; Totenhagen, J.; Sherwood, J.; Qin, Y.; Gurler, D.; Bolding, M. S.; Bao, Y. Ultrathin Iron Oxide Nanowhiskers as Positive Contrast Agents for Magnetic Resonance Imaging. *Adv. Funct. Mater.* **2015**, *25*, 490−494.
(51) Noh, S. H.; Na, W.; Jang, J. T.; Lee, J. H.; Lee, E. J.; Moon, S. H.; Lim, Y.; Shin, J. S.; Cheon, J. Nanoscale Magnetism Control via Surface and Exchange Anisotropy for Optimized Ferrimagnetic Hysteresis. *Nano Lett.* **2012**, *12*, 3716−21.
(52) Balasubramaniam, S.; Kayandan, S.; Lin, Y. N.; Kelly, D. F.; House, M. J.; Woodward, R. C.; St Pierre, T. G.; Riffle, J. S.; Davis, R. M. Toward Design of Magnetic Nanoparticle Clusters Stabilized by Biocompatible Diblock Copolymers for T(2)-Weighted MRI Contrast. *Langmuir* **2014**, *30*, 1580−7.
(53) Peiris, P. M.; Toy, R.; Abramowski, A.; Vicente, P.; Tucci, S.; Bauer, L.; Mayer, A.; Tam, M.; Doolittle, E.; Pansky, J.; et al. Treatment of Cancer Micrometastasis Using a Multicomponent Chain-Like Nanoparticle. *J. Controlled Release* **2014**, *173*, 51−8.
(54) Peiris, P. M.; Toy, R.; Doolittle, E.; Pansky, J.; Abramowski, A.; Tam, M.; Vicente, P.; Tran, E.; Hayden, E.; Camann, A.; et al. Imaging Metastasis Using an Integrin-Targeting Chain-Shaped Nanoparticle. *ACS Nano* **2012**, *6*, 8783−8795.
(55) Rahmer, J.; Halkola, A.; Gleich, B.; Schmale, I.; Borgert, J. First Experimental Evidence of the Feasibility of Multi-Color Magnetic Particle Imaging. *Phys. Med. Biol.* **2015**, *60*, 1775−91.

DOI: 10.1021/acs.jpclett.5b00610
J. Phys. Chem. Lett. 2015, 6, 2509−2517